AJNR

Three-Dimensional Dynamic MR Digital Subtraction Angiography Using Sensitivity Encoding for the Evaluation of Intracranial Arteriovenous Malformations: A Preliminary Study

Jean-Yves Gauvrit, Xavier Leclerc, Catherine Oppenheim, Thierry Munier, Denis Trystram, Henda Rachdi, François Nataf, Jean-Pierre Pruvo and Jean-François Meder

AJNR Am J Neuroradiol 2005, 26 (6) 1525-1531
http://www.ajnr.org/content/26/6/1525

Three-Dimensional Dynamic MR Digital Subtraction Angiography Using Sensitivity Encoding for the Evaluation of Intracranial Arteriovenous Malformations: A Preliminary Study

Jean-Yves Gauvrit, Xavier Leclerc, Catherine Oppenheim, Thierry Munier, Denis Trystram, Henda Rachdi, François Nataf, Jean-Pierre Pruvo, and Jean-François Meder

BACKGROUND AND PURPOSE: **Our aim was to develop 3D dynamic MR digital subtraction angiography with high temporal resolution without sacrificing spatial resolution by using sensitivity encoding for the evaluation of cerebral arteriovenous malformations.**

METHODS: **Nineteen patients with 19 angiographically proven arteriovenous malformations (16 supratentorial and 3 infratentorial) were assessed by conventional catheter angiography and 3D dynamic MR digital subtraction angiography. A 3D contrast-enhanced gradient-echo sequence with sensitivity encoding based on a parallel imaging technique was performed and acquired 20 dynamic images, repeated 18 times every 1.7 seconds. Three-dimensional dynamic MR digital subtraction angiograms were analyzed independently by two radiologists in a blinded fashion with regard to arteriovenous malformation nidus and venous drainage. Conventional catheter angiography was used as reference.**

RESULTS: **All MR imaging examinations were assessable. Interobserver agreement was excellent for the detection of nidus and for the evaluation of nidus size ($\kappa = 1$ and 0.875, respectively) but moderate for the visualization of the venous drainage ($\kappa = 0.56$). All nidi detected on conventional catheter angiography were clearly depicted on 3D dynamic MR digital subtraction angiography. The evaluation of the size of the nidus by both techniques was similar. On 3D dynamic MR angiograms, veins were correctly analyzed in 17 of 19 arteriovenous malformations.**

CONCLUSION: **Our preliminary study demonstrates that 3D dynamic MR digital subtraction angiography using sensitivity encoding with a high spatial resolution is appropriate for the assessment of arteriovenous malformations.**

MR angiography with high spatial resolution is used as a noninvasive alternative to conventional angiography for the assessment of cerebral arteriovenous malformations. The 3D time-of-flight technique is considered the method of reference for the noninvasive assessment of intracranial vasculature. In cases of cerebral arteriovenous malformation, this technique is useful for the evaluation of feeding arteries and for the detection of extranidal aneurysms (1, 2). However, accurate delineation of the nidus and venous drainage remains poor on 3D time-of-flight MR angiography because of saturation effects that may be responsible for a decreased signal intensity in capillaries and veins.

Two-dimensional dynamic MR digital subtraction angiography has recently been developed to circumvent this drawback. It combines the T1 shortening effect of gadolinium, subsecond images, and the digital subtraction technique, allowing high temporal resolution MR angiograms (1–5). It provides hemodynamic information similar to that obtained by conventional catheter angiography with separation of arterial and venous phases of angiography. Previous reports showed the potential interest in 2D dynamic

Received September 13, 2004; accepted after revision December 3.

From the Department of Neuroradiology (J.-Y.G., X.L., H.R., J.-P.P.), EA 2691, Roger Salengro Hospital, University Hospital of Lille, Lille, France; the Departments of Neuroradiology (C.O., D.T., J.-F.M.) and Neurosurgery (F.N.), Sainte-Anne Hospital, Paris V University, Paris, France; and General Electric Healthcare Technologies (T.M.), Buc, France.

Address correspondence and reprints to Jean-Yves Gauvrit, Department of Neuroradiology, EA 2691, Roger Salengro Hospital, University Hospital of Lille, Lille, France (e-mail: jygauvrit@chru-lille).fr

MR digital subtraction angiography for the diagnosis of arteriovenous malformations and for follow-up of stereotactic radiosurgery (1, 2, 4, 6–8). In particular, MR imaging plays an important role in the evaluation of the decrease of nidus size and/or disappearance of venous drainage.

Two-dimensional dynamic MR digital subtraction angiography has also been successfully used for the identification, classification, and follow-up of dural arteriovenous fistulas (2, 6, 9–11) and for the depiction of cervical and intracranial arteries (12). However, this method has several limitations, including poor visualization of small vessels or shunts because of partial volume effects, 2D acquisition with a large section thickness, and limited spatial resolution. Recent developments using multiple surface coils and parallel imaging methods such as sensitivity encoding allow a decrease in imaging time and the maintenance of spatial resolution (13–18). Current clinical applications, such as imaging of arteriovenous malformation nidus and venous drainage, that can benefit from these techniques mainly require sequential repeated images of the same plane with optimization of temporal resolution.

In this preliminary study, we investigate a 3D dynamic MR digital subtraction angiography sequence combining sensitivity and gradient encoding for arteriovenous malformation assessment.

Methods

Subjects

From September 2003 to March 2004, 45 consecutive patients underwent conventional catheter angiography for a cerebral arteriovenous malformation. Only patients with a nidus size 1 cm and without residual arteriovenous fistulas were included. In fact, 19 patients (10 men and 9 women; age range, 19–62 years; mean age, 37 years) were studied and underwent conventional catheter angiography and 3D dynamic MR digital subtraction angiography with a time interval between examinations of <48 hours. Sixteen arteriovenous malformations were located on the supratentorial circulation (6 frontal, 2 parietal, 3 temporal, 3 occipital, 1 basal ganglia, and 1 corpus callosum) and 3 on the infratentorial circulation. The neurological initial presentation was intracranial hemorrhage (4 cases), seizure (3 cases), and headache (3 cases) (2). The remaining patients (10 cases) were asymptomatic.

Twelve patients had one patent arteriovenous malformation without previous treatment. The remaining 7 cases had arteriovenous malformations partially obliterated after an embolization treatment (3 cases), linear accelerator radiosurgery (3 cases), or both treatments (1 case). Posttreatment studies were performed from an average of 35 months (range, 12–61 months) after the radiosurgery (19).

MR Imaging

MR imaging was performed on a 1.5-T superconducting system (Signa Excite Echospeed, GE Healthcare, Waukesha, WI) with 33 mT/m gradient strength, used in conjunction with a multi-elements head coil with an 8-channel-receiver radiofrequency system. Patients were positioned with a 20-gauge intravenous catheter inserted into the antecubital vein. All patients were referred for MR imaging in line with accepted clinical practices at our institution. Routine MR imaging including pre- and postcontrast T1-weighted spin-echo and T2-weighted fast spin-echo imaging was performed.

Three-dimensional dynamic MR digital subtraction angiography with array spatial sensitivity encoding techniques was performed in the sagittal and coronal planes. Twenty dynamic images were obtained to track the contrast bolus. One frame of 20 dynamic images per 1.7 seconds was repeated 18 times. Imaging parameters for the dynamic images were the following: TR\TE\flip angle, 3.6\1.4\25°; 300×300 mm field of view; 320×192 acquisition matrix; section thickness of 10 mm with 20 overlapped sections resulting in a 10-cm-thick volume; and a 166.6-kHz bandwidth. Spatial resolution was $0.9375 \times 1.562 \times 10$ mm^3 and $0.58 \times 0.58 \times 5$ mm^3 after zero-filling interpolation. The coil was used for fourfold array spatial sensitivity encoding techniques reduction along the left–right phase-encoding direction for coronal scanning and along the anteroposterior phase encoding direction for sagittal scanning. Three-dimensional dynamic MR digital subtraction angiography was initiated 5 seconds after the start of a 10-mL gadolinium (Dotarem, Guerbet, France) bolus administered intravenously at a rate of 3 mL/s using a Spectris power injector (Medrad, Indianola, PA) followed by a 10-mL saline flush. A separate contrast bolus was used for each anatomic plane. MR angiographic source images were transferred to a workstation (Advantage Windows 4.1, GE Healthcare, Buc, France). Image processing included subtraction of the first volume from the series and reconstruction of the maximum intensity projection obtained and consisted of lateral and anteroposterior projections. The time required for each examination was about 12 minutes, including 2 minutes for both acquisitions (sagittal and coronal) and 10 minutes to generate subtracted angiographic images.

Conventional Catheter Angiography

Conventional catheter angiography was performed within 2 days after 3D dynamic MR digital subtraction angiography (Integris BV3000, Philips Medical Systems, Best, the Netherlands), with a 4-French catheter via a femoral artery approach with a filming rate of 2 and 3 images per second. Follow-up angiography included a selective injection of internal and common carotid or vertebral arteries in the frontal and sagittal views completed by additional views when necessary. Images were printed with a 512×512 matrix and a field of view of 17 cm. For each projection, an 8- to 16-mL bolus of iodinated contrast material (iobitridol, Xenetix, Guerbet, France) was injected at a rate of between 3 and 6 mL/s using a power injector.

Image Evaluation

Two neuroradiologists (C.O., J.-Y.G.), both blinded to the results of either study but with knowledge of the medical history and the clinical score, independently reviewed the 3D dynamic MR digital subtraction angiography images. The observers were blinded to the conventional catheter angiography results. Conventional angiograms were reviewed by two other neuroradiologists (H.R., J.-F.M.), who were unaware of the 3D dynamic MR digital subtraction angiography findings.

Three-dimensional dynamic MR digital subtraction angiography image contrast was graded as low when the signal intensity in the enhanced arterial lumen was only slightly higher than the signal intensity in the background, moderate when the signal intensity was clearly higher, and high when the signal intensity was optimal: in this case, each structure (feeding artery, portion of nidus, vein) was clearly localized on MR angiography in a way similar to that on the conventional catheter angiography images (20).

Cerebral arteriovenous malformation size was analyzed in 3 projections (craniocaudal, anteroposterior, and lateral views), but only the largest dimension of the nidus was provided according to Spetzler and Martin's classification (21) and then was classified into 1 of 3 groups: small (<3 cm, medium (3–6 cm), and large (>6 cm).

The venous drainage of arteriovenous malformations was recorded as deep, superficial, or superficial and deep. We

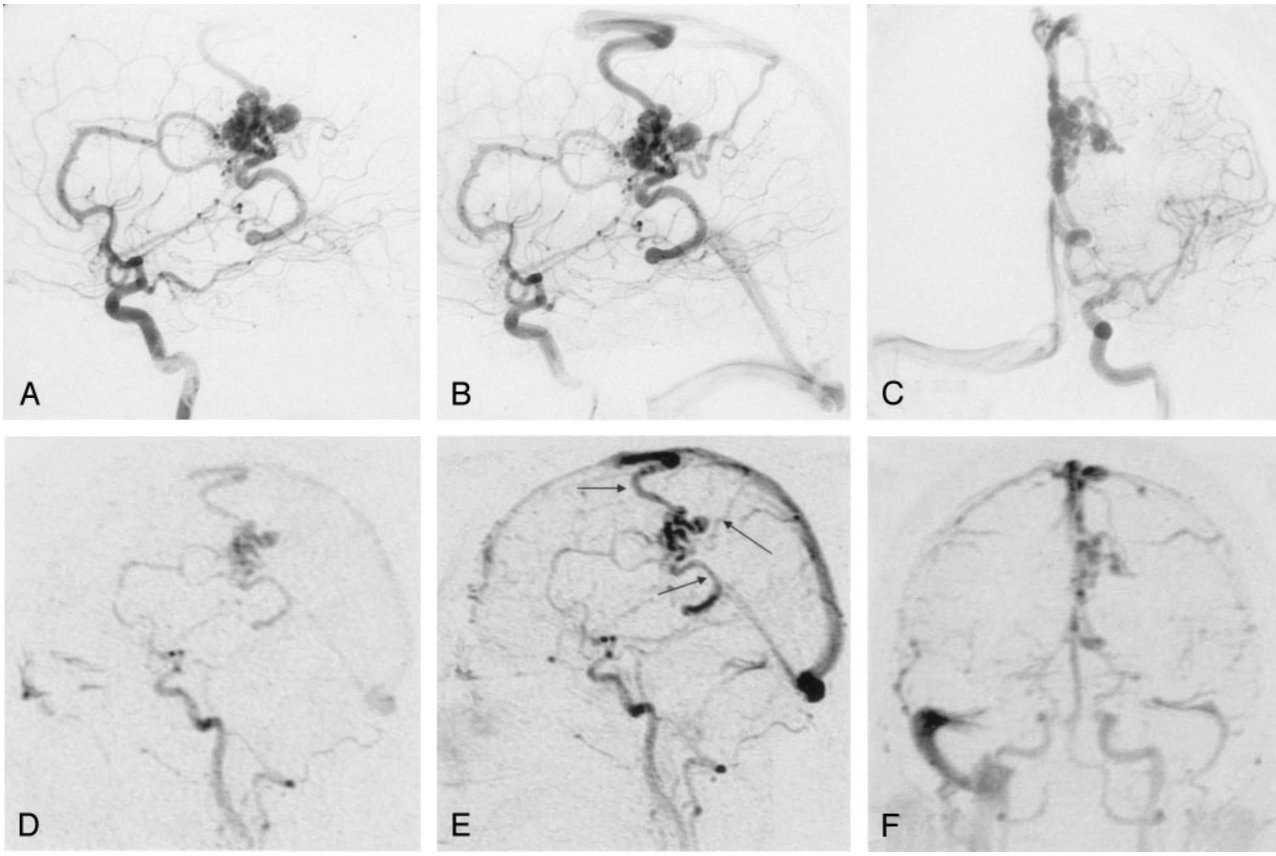

FIG 1. 31-year-old man with a left frontal arteriovenous malformation.

A–C, Conventional angiograms in sagittal (*A, B*) and coronal (*C*) views show an arteriovenous malformation fed by branches of the anterior cerebral artery. It drains into the superior sagittal sinus via 2 veins and into the right sinus via 1 deep vein.

D–F, Several stages of 3D dynamic MR digital subtraction angiograms during the passage of contrast bolus in sagittal (*D,* late arterial phase; *E,* venous phase) and coronal (*F,* venous phase) maximum-intensity-projection reconstructions show findings similar to those of the conventional catheter angiography with 3 draining veins (arrows, *E*).

defined the drainage as "superficial" when veins drained into the cortical venous system and as "deep" when veins drained into the vein of Galen or the straight sinus.

Statistical Analysis

All statistical studies were performed using MedCalc software (Mariakerke, Belgium). The first step of the analysis was an evaluation of the level of interobserver agreement for each set of 3D dynamic MR digital subtraction angiograms by means of the κ statistic. The second step consisted of a comparison between 3D dynamic MR digital subtraction angiograms and conventional catheter angiograms for the detection of nidus and venous drainage and for the evaluation of the size of the nidus using the same statistical tests. Kappa values 0.6 suggested a substantial agreement, and values 0.8 indicated an excellent agreement. *P* values $<.05$ were regarded as significant.

Results

On conventional catheter angiography, 19 arteriovenous malformations were seen in 19 patients. No patient had multiple arteriovenous malformations. Nineteen nidi were clearly demonstrated on conventional catheter angiography.

Image Quality

Successful 3D dynamic MR digital subtraction angiograms were obtained in all patients. The overall image quality of 3D dynamic MR digital subtraction angiograms was judged high in 18 patients and moderate in 1 patient; the moderate quality did not prevent interpretation.

Interobserver Agreement

Interobserver agreement was excellent for nidus detection and nidus size, (κ = 1 and 0.875, P = .22, respectively) and moderate for the venous drainage (κ = 0.56, P = .12). Discrepancies between the 2 examiners were noted in 1 case for the evaluation of nidus size and in 5 cases for the visualization of venous drainage. In these cases, an additional reading by both examiners was performed to reach a consensus.

Intertechnique Agreement (Figs 1–2)

As indicated in Table 1, of the 19 arteriovenous malformations assessed in 19 patients, 19 nidi were clearly demonstrated on 3D dynamic MR digital subtraction angiography.

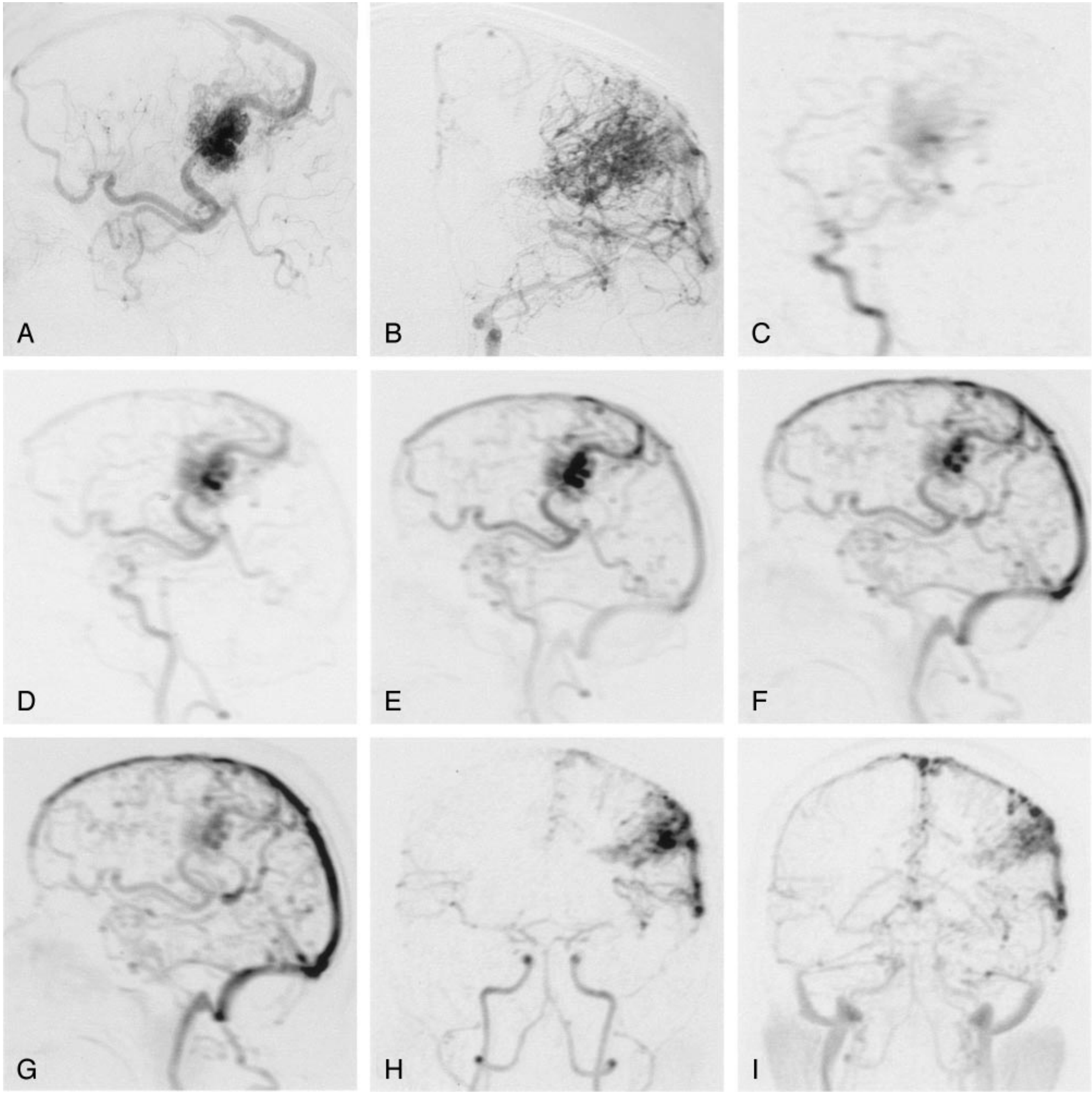

FIG 2. Postradiosurgery study of 48-year-old woman with a left frontal arteriovenous malformation.

A–B, Conventional angiograms in sagittal (*A*) and coronal (*B*) views show a medium-sized arteriovenous malformation fed by branches of the middle cerebral artery. It drains via 2 veins (anterior and posterior) into the superior sagittal sinus. Note stenosis of the anterior vein.

C–I, Several stages of 3D dynamic MR digital subtraction angiograms during the passage of a contrast bolus in sagittal (*C*, early arterial phase; *D*, late arterial phase; *E,* early venous phase; and *F–G,* late venous phase) and coronal (*H*, arterial phase; *I,* early venous phase) maximum-intensity-projection reconstructions show the nidus and 2 draining veins matching the conventional catheter angiography findings.

Nidus Size

There was complete agreement ($\kappa = 1$) between conventional catheter angiography and 3D dynamic MR digital subtraction angiography for classification of nidus size: 14 nidi were classified as small, 4 as medium, and 1 as large.

Venous Drainage

Of 19 arteriovenous malformations, conventional catheter angiography showed deep venous drainage in 11 cases and exclusively superficial drainage in 8. Three-dimensional dynamic MR digital subtraction angiography findings showed a good agreement with conventional catheter angiography in 17 cases ($\kappa = 0.84$, $P = .1$). In 1 case, 3D dynamic MR digital subtraction angiography misidentified superficial venous drainage as deep drainage, and in 1 case, 3D dynamic MR digital subtraction angiography incorrectly showed superficial venous drainage, whereas conventional catheter angiography demonstrated only deep venous drainage.

Summary of CCA and 3D dynamic MR-DSA findings

Parameters	CCA	3D dynamic MR-DSA
Detection of nidus	19/19	19/19
Size of nidus		
<3 cm	14/19	14/19
3–6 cm	4/19	4/19
>6 cm	1/19	1/19
Venous drainage		
superficial	8/19	7/19
deep	3/19	3/19
deep and superficial	8/19	9/19

Discussion

Our study showed 3D dynamic contrast-enhanced MR angiography to be highly sensitive for the detection of arteriovenous malformation nidus and for determining nidus measurements according to Spetzler and Martin's classification (21). Of 19 patients with an angiographically proven nidus, 3D dynamic MR digital subtraction angiography showed similar findings in all cases.

The standard technique of contrast-enhanced 3D MR angiography is based on a single acquisition of the imaging volume during the peak of maximum concentration of gadolinium within the arteries. This provides high contrast of images with minimized flow-related artifacts. However, a major drawback of this technique, because of the impossibility of repeating sequences with a short time acquisition during the passage of the contrast agent, is the absence of hemodynamic information on the different phases of the intracranial circulation; this point is crucial for the evaluation of brain arteriovenous malformations (22, 23). To circumvent this issue, time-resolved 3D MR angiography has been developed, and preliminary reports suggest that this method constitutes a potential tool for the follow-up of patients with cerebral arteriovenous malformations (2, 14, 24–26).

Two-dimensional dynamic time-resolved MR digital subtraction angiography has proven its effectiveness for the evaluation of arteriovenous malformations (7, 9, 10, 26, 27). However limitations of this technique include the low spatial resolution ($1 \times 2 \times 80$ mm) that is responsible for a poor visualization of small vessels or shunts due to partial-volume effects. Other MR angiographic techniques with or without contrast, namely time of flight or phase contrast, have great value for the assessment of arteriovenous malformations. These techniques with higher spatial resolution lack the temporal resolution to optimally reflect high-flow cerebral vascular malformations and to distinguish nidus from draining veins, both of which are important for the diagnosis of arteriovenous malformations (28, 29).

New technical developments using parallel imaging such as sensitivity encoding (13), array spatial sensitivity encoding technique (30), or simultaneous acquisition of spatial harmonics (16, 17) can provide high spatial and temporal resolution. The use of parallel imaging techniques is appropriate for contrast MR angiography because the relatively high signal intensity level can be exploited for improving spatial resolution while preserving a short scan duration (31); consequently, the successive phases of the bolus can be visualized, a step essential for the analysis of arteriovenous malformations (18).

Three-dimensional dynamic MR digital subtraction angiography using parallel imaging entails the following steps: acquisition of sensitivity maps before the intravenous administration of contrast agent, acquisition of dynamic reduced-field-of-view data during the passage of the contrast bolus, reconstruction of reduced-field-of-view images, unfolding of reduced-field-of-view images, subtraction of the first volume from all successive ones, and creation of general or targeted maximum intensity projections (32). The 3D dynamic MR digital subtraction angiography with sensitivity encoding techniques has potential advantages over 2D dynamic MR digital subtraction angiography for the evaluation of intracranial vascular malformations. First, MR angiography with sensitivity encoding is a 3D ultrafast MR imaging technique. It uses multiple receiver coils and exploits information related to the distinct spatial sensitivity of each element of the coil and fast parallel-encoding imaging techniques. This technical development with the unique geometry of phased-array coils spatially encodes the image faster; the speed improvement depends on a factor equal to the number of parallel receiver coils used. Thus, our sequence provided time resolving[8] to 1.7 seconds because of an array spatial sensitivity encoding techniques factor set to 4. MR angiography with this time reduction is better suited to the exploration of arteriovenous malformations, thus facilitating the understanding of intracranial hemodynamics.

Second, the array spatial sensitivity encoding technique may be used to improve spatial resolution ($0.58 \times 0.58 \times 5$ mm^3) compared with 2D dynamic MR digital subtraction angiography. Our sequence provided 3D dynamic cerebral MR angiography with submillimeter in-plane resolution, with a section thickness of 5 mm. The simultaneous increase of both spatial and temporal resolution compared with that of a previous study using 2D dynamic MR digital subtraction angiography might explain the higher interobserver agreement for the evaluation of feeding arteries and draining veins (6).

Third, irrespective of the arteriovenous malformation size, coverage of 10 cm was always sufficient to image the whole arteriovenous malformation without view sharing or temporal interpolation.

Fourth, as with the 2D technique, 3D acquisition did not require an increase in contrast media because a small volume of contrast medium (10 mL) is sufficient for each plane. Partial k-space updating for each dynamic image is used to shorten the acquisition time. The duration of the plateau concentration of contrast agent is maintained at least over the duration of multiple dynamic acquisitions used in view sharing and interpolation (33). Hence, at a fixed injection rate and a similar dynamic acquisition time, parallel imaging techniques require less contrast agent to maintain appropriate vessel opacification (34).

A limiting factor of our technique is the use of a large field of view of 300 mm, thus decreasing the pixel size. However, increasing the field of view was necessary to obtain an acceleration factor of 4. With a smaller field of view, a factor of only 2 may be used, leading to a lower temporal resolution. The parallel imaging technique allows scan time to be reduced, although this is to the detriment of the signal-to-noise ratio (34). The loss in signal -to-noise ratio is equivalent to the square root of the reduction in acquisition time. Thus, a scan with an accelerator factor of 4 requires one quarter of the imaging time for a given resolution, but with $\sqrt{1/4}$ or 50% of the signal-to-noise ratio. To improve the signal-to-noise ratio, we reduced the readout bandwidth and slightly increased the field of view to 300 mm and the injection rate of the contrast agent to 3 mL/s (33).

Another limitation of the technique is an aliasing artifact affecting the periphery of the field of view and resulting in an overlap of the arteries and veins. This artifact is due to the geometry of the receiver coils. In our study, no artifact occurred with the use of a phased-array coil optimized for parallel imaging.

Finally, the temporal resolution on 3D dynamic MR digital subtraction angiography sequences remains limited with 1 frame per 1.7 seconds compared with 1 frame per 0.5 seconds with conventional catheter angiography. This may explain the low reproducibility of this technique for the assessment of venous drainage, especially in case of slow flow or residual small fistulas.

Recent studies have used 3D MR angiography acquisition and parallel imaging for the assessment of supraaortic extracranial or peripheral vessels or abdominal vasculature (14, 15, 33, 34). The results showed the ability of this technique to enhance spatial ($1.0 \times 2.0 \times 4.0$ mm^3) and temporal resolution (4 seconds) in a clinical setting. One study (30) evaluated 2D dynamic MR digital subtraction angiography using sensitivity encoding techniques in the assessment of intracranial hemodynamics with an improved temporal resolution and showed that this technique could provide satisfactory examinations in patients with arteriovenous malformations. In that study, however, spatial resolution was poor because of the 2D acquisition, and maximum-intensity-projection reconstructions were not assessed.

Other techniques may be used to decide the therapeutic strategy. Recently, it has been shown that CT angiography including the newest scanners and subsecond cine function may be used to define the treatment planning and especially for the stereotactic location of the nidus before surgical resection or radiosurgical treatment (35).

Further optimization of the imaging sequence will be undertaken to improve the image quality. This will probably be achieved by combining an increased injection rate and a smaller imaging duration–bolus duration ratio (33, 36, 37). Three-dimensional dynamic MR digital subtraction angiography with parallel imaging techniques might replace conventional catheter angiography in certain circumstances and especially for treatment planning and follow-up of patients with cerebral arteriovenous malformations. Our study suggests that cerebral arteriovenous malformations may be controlled by 3D dynamic MR digital subtraction angiography after treatment by radiosurgery as long as an opacification of the nidus or an early venous drainage persists. When MR angiograms no longer show the nidus or a draining vein, conventional catheter angiography is performed to confirm the complete occlusion of the nidus or the presence of a residual fistula. Moreover, this technique may improve the etiological MR imaging work-up of hematomas in young patients (38).

Conclusion

Our preliminary study demonstrates that the 3D dynamic MR digital subtraction angiography using sensitivity encoding technique is suited for the evaluation of arteriovenous malformation and can provide essential information such as the size of the nidus and the presence of venous drainage. It allows an increased temporal resolution without sacrificing spatial resolution and provides adequate imaging coverage.

References

1. Griffiths PD, Hoggard N, Warren DJ, Wilkinson ID, Anderson B, Romanowski CA. **Brain arteriovenous malformations: assessment with dynamic MR digital subtraction angiography**. *AJNR Am J Neuroradiol* 2000;21:1892–1899
2. Klisch J, Strecker R, Hennig J, Schumacher M. **Time-resolved projection MRA: clinical application in intracranial vascular malformations**. *Neuroradiology* 2000;42:104–107
3. Aoki S, Yoshikawa T, Hori M, et al. **Two-dimensional thick-slice MR digital subtraction angiography for assessment of cerebrovascular occlusive diseases**. *Eur Radiol* 2000;10:1858–1864
4. Tsuchiya K, Katase S, Yoshino A, Hachiya J. **MR digital subtraction angiography of cerebral arteriovenous malformations**. *AJNR Am J Neuroradiol* 2000;21:707–711
5. Wang Y, Johnston DL, Breen JF, et al. **Dynamic MR digital subtraction angiography using contrast enhancement, fast data acquisition, and complex subtraction**. *Magn Reson Med* 1996;36:551–556
6. Aoki S, Yoshikawa T, Hori M, et al. **MR digital subtraction angiography for the assessment of cranial arteriovenous malformations and fistulas**. *AJR Am J Roentgenol* 2000;175:451–453
7. Mori H, Aoki S, Okubo T, et al. **Two-dimensional thick-slice MR digital subtraction angiography in the assessment of small to medium-size intracranial arteriovenous malformations**. *Neuroradiology* 2003;45:27–33
8. Warren DJ, Hoggard N, Walton L, et al. **Cerebral arteriovenous malformations: comparison of novel magnetic resonance angiographic techniques and conventional catheter angiography**. *Neurosurgery* 2001;48:973–982; discussion 982–973
9. Coley SC, Romanowski CA, Hodgson TJ, Griffiths PD. **Dural arteriovenous fistulae: noninvasive diagnosis with dynamic MR digital subtraction angiography**. *AJNR Am J Neuroradiol* 2002;23:404–407
10. Noguchi K, Melhem ER, Kanazawa T, Kubo M, Kuwayama N, Seto H. **Intracranial dural arteriovenous fistulas: evaluation with combined 3D time-of-flight MR angiography and MR digital subtraction angiography**. *AJR Am J Roentgenol* 2004;182:183–190
11. Wetzel SG, Bilecen D, Lyrer P, et al. **Cerebral dural arteriovenous fistulas: detection by dynamic MR projection angiography**. *AJR Am J Roentgenol* 2000;174:1293–1295
12. Wetzel SG, Haselhorst R, Bilecen D, et al. **Preliminary experience with dynamic MR projection angiography in the evaluation of cervicocranial steno-occlusive disease**. *Eur Radiol* 2001;11:295–302
13. Pruessmann KP, Weiger M, Scheidegger MB, Boesiger P. **SENSE: sensitivity encoding for fast MRI**. *Magn Reson Med* 1999;42:952–962

14. Weiger M, Pruessmann KP, Kassner A, et al. **Contrast-enhanced 3D MRA using SENSE**. *J Magn Reson Imaging* 2000;12:671–677
15. Golay X, Pruessmann KP, Weiger M, et al. **PRESTO-SENSE: an ultrafast whole-brain fMRI technique**. *Magn Reson Med* 2000;43:779–786
16. Sodickson DK, McKenzie CA, Li W, Wolff S, Manning WJ, Edelman RR. **Contrast-enhanced 3D MR angiography with simultaneous acquisition of spatial harmonics: a pilot study**. *Radiology* 2000;217:284–289
17. Sodickson DK, Manning WJ. **Simultaneous acquisition of spatial harmonics (SMASH): fast imaging with radiofrequency coil arrays**. *Magn Reson Med* 1997;38:591–603
18. Chen Q, Quijano C, Mai V, et al. **On improving temporal and spatial resolution of 3D contrast-enhanced body MR angiography with parallel imaging.** *Radiology* 2004;231:893–899
19. Meder JF, Oppenheim C, Blustajn J, et al. **Cerebral arteriovenous malformations: the value of radiologic parameters in predicting response to radiosurgery.** *AJNR Am J Neuroradiol* 1997;18:1473–1483
20. Farb RI, McGregor C, Kim JK, et al. **Intracranial arteriovenous malformations: real-time auto-triggered elliptic centric-ordered 3D gadolinium-enhanced MR angiography–initial assessment**. *Radiology* 2001;220:244–251
21. Spetzler R, Martin N. **A proposed grading system for arteriovenous malformations**. *J Neurosurg* 1986;65:476–483
22. Korosec FR, Frayne R, Grist TM, Mistretta CA. **Time-resolved contrast-enhanced 3D MR angiography**. *Magn Reson Med* 1996;36:345–351
23. Prince MR, Yucel EK, Kaufman JA, Harrison DC, Geller SC. **Dynamic gadolinium-enhanced three-dimensional abdominal MR arteriography**. *J Magn Reson Imaging* 1993;3:877–881
24. Barger AV, Block WF, Toropov Y, Grist TM, Mistretta CA. **Time-resolved contrast-enhanced imaging with isotropic resolution and broad coverage using an undersampled 3D projection trajectory**. *Magn Reson Med* 2002;48:297–305
25. Carroll TJ. **The emergence of time-resolved contrast-enhanced MR imaging for intracranial angiography**. *AJNR Am J Neuroradiol* 2002;23:346–348
26. Shim YW, Chung TS, Kang WS, Joo JY, Strecker R, Hennig J. **Non-invasive follow-up evaluation of post-embolized AVM with time-resolved MRA: a case report**. *Korean J Radiol* 2002;3:271–275
27. Hennig J, Scheffler K, Laubenberger J, Strecker R. **Time-resolved projection angiography after bolus injection of contrast agent**. *Magn Reson Med* 1997;37:341–345
28. Kesava P, Turski P. **Magnetic resonance angiography of vascular malformations.** *Magn Reson Imaging Clin N Am* 1998;6:811–833
29. Duran M, Schoenberg SO, Yuh WT, Knopp MV, van Kaick G, Essig M. **Cerebral arteriovenous malformations: morphologic evaluation by ultrashort 3D gadolinium-enhanced MR angiography**. *Eur Radiol* 2002;12:2957–2964. Epub 2002 Jun 4
30. Mori H, Aoki S, Masumoto T, et al. **Two-dimensional magnetic resonance digital substraction angiography using array spatial sensitivity encoding techniques in the assessment of intracranial hemodynamics**. *Radiat Med* 2002;20:223–229
31. Gaa J, Weidauer S, Requardt M, Kiefer B, Lanfermann H, Zanella FE. **Comparison of intracranial 3D-ToF-MRA with and without parallel acquisition techniques at 1.5T and 3.0T: preliminary results**. *Acta Radiol* 2004;45:327–332
32. Pruessmann KP, Weiger M, Boesiger P. **Sensitivity encoded cardiac MRI**. *J Cardiovasc Magn Reson* 2001;3:1–9
33. Frayne R, Grist TM, Swan JS, Peters DC, Korosec FR, Mistretta CA. **3D MR DSA: effects of injection protocol and image masking**. *J Magn Reson Imaging* 2000;12:476–487
34. Paschal CB, Morris HD. **K-space in the clinic**. *J Magn Reson Imaging* 2004;19:145–159
35. Sanelli PC, Mifsud MJ, Stieg PE. **Role of CT angiography in guiding management decisions of newly diagnosed and residual arteriovenous malformations**. *AJR Am J Roentgenol* 2004;183:1123–1126
36. Maki JH, Prince MR, Londy FJ, Chenevert TL. **The effects of time varying intravascular signal intensity and k-space acquisition order on three-dimensional MR angiography image quality**. *J Magn Reson Imaging* 1996;6:642–651
37. Maki JH, Prince MR, Chenevert TC. **Optimizing three-dimensional gadolinium-enhanced magnetic resonance angiography: original investigation**. *Invest Radiol* 1998;33:528–537
38. Leclerc X, Khalil C, Silvera S, et al. **Imaging of non-traumatic intracerebral hematoma**. *J Neuroradiol* 2003;30:303–316